Localization of Volcanic Activity: Topographic Effects on Dike Propagation, Eruption and Conduit Formation

Edward S. Gaffney[a*] and Branko Damjanac[b]

[a]Gaffney Associates, Inc., Glenwood, IA 51534 USA edgaffney@earthlink.net

[b]Itasca Consulting Group, Minneapolis, MN 55401 USA

[*]Corresponding author

Abstract

Magma flow in a dike rising in a crack whose strike runs from a highland or a ridge to an adjacent lowland has been modelled to determine the effect of topography on the flow. It is found that there is a distinct tendency for the flow to be diverted away from the highland end of the strike toward the lowland. Separation of the geometric effect of the topography from its effect on lateral confining stresses on the crack indicates that both contribute to the effect but that the effect of stress is less important. Although this analysis explains a tendency for volcanic eruptions to occur in low lands, it does not preclude eruptions on highlands. The particular configuration modelled mimics topography around the proposed nuclear waste repository at Yucca Mountain, Nevada, so that the results may indicate some reduction in the volcanic hazard to the site.

Introduction

The propagation of dikes has been the subject of analysis by geoscientists for decades. Most of this work deals with dike propagation far from the surface (e.g., Pollard and

Muller (1976); Spence and Turcotte (1990); Lister, 1990a, 1990b, 1991, Lister and Kerr, 1991). Much of the mathematical basis for these studies is shared with analysis of hydraulic fractures used to stimulate oil or gas production (Perkins and Kern, 1961; Howard and Fast 1958; Geertsma and de Klerk, 1969).

Interaction of a dike with the surface complicates the problem considerably due to the rapid reduction in lateral confinement as the crack tip nears the surface. Pollard and Holzhausen (1979) analyzed the mechanical interaction of a dike with a free surface, and Brandsdottir and Einarsson (1979) described seismic activity associated with the 1977 deflation of Krafla. Pollard et al. (1983) discussed how dike propagation can alter surface topography in volcanic rift zones. Rubin analyzed similar problems of surface deformation by dike propagation (e.g., Rubin and Pollard, 1988; Rubin, 1990; Rubin, 1992).

This paper addresses not how dike propagation modifies the surface, but how the presence and nature of the surface affect the dike propagation. The effect of the free surface on hydrofracture propagation has been addressed by Zhang et al. (2002), who investigated the propagation of a penny-shaped fracture parallel to a free surface with applicability to longwall coal mining. Pinel and Jaupart (2004) found that dikes propagating radially from beneath an edifice will remain at depth until they reach the edge of the edifice, by which point they will begin to rise toward the surface. The present paper considers the effect of topography on the vertical propagation of a planar dike in the vicinity of a topographic ridge with a different strike than that of the dike.

Flow in Dike Nearing Surface

We tested the hypothesis that magma in a dike whose center along strike was on the edge of a topographic high would be diverted toward the adjacent lowlands as illustrated schematically in Figure 1. Because the aperture of a dike is greater near its center than at the ends of its strike, magma would be expected to rise higher at the center of the strike length than at the edge. Thus, if magma reached the surface in a valley, pressure driving magma upward under the mountain could be relieved before magma rose as high as the bottom of the canyon. Halted under the mountain, magma there would begin to solidify and the eruption would be localized in the canyon.

To test this hypothesis, we use the three-dimensional hydromechanical code FLAC3D. This code is used primarily for simulation of the mechanical response of geologic structures to groundwater movement through pore space and does not simulate crack propagation *per se*. Rather, we are interested in magma flowing in a small-aperture predetermined crack and propping it open in response to the fluid pressure in the crack. Use of this approach to simulate dike propagation is justified by the fact that the megascopic fracture toughness of rock masses is small (Spence and Turcotte 1985). In order to model fluid flow in an open crack, the crack was represented as a single row of cells of thickness, d. The dike aperture was not explicitly represented in the model because it is zero initially, and even when the dike opens due to magma injection it will be much smaller than any characteristic length of the model. The aperture, a, is calculated during the simulation as a function of model deformation. The permeability tensor of each zone is adjusted at each time step in response to the pressure in the zone according to the relationship

$$k_{ij} = \delta_{ij} \frac{a^3}{12\mu d}, \tag{1}$$

which is obtained by equating the flow through a layer of permeable zones of thickness d from Darcy's law

$$Q_i = d\, k_{ij} \frac{\partial(p - \rho_f z g)}{\partial x_j}, \tag{2}$$

with the flow in a crack of width a from the Poiseuille law

$$Q_i = \frac{a^3}{12\mu} \delta_{ij} \frac{\partial(p - \rho_f z g)}{\partial x_j} \tag{3}$$

under the same gradient. Here, δ_{ij} is the Kronecker delta, a is the aperture of the crack, μ is the viscosity of the fluid, p is the pressure, ρ_f is the density of the fluid, z is the depth from the surface, and g is the acceleration of gravity. In equations (2) and (3), repeated indices are summed. With this adjustment to the permeability, the value of d has no effect on the model solution.

Preliminary analyses demonstrated that a square block-shaped model with the edge length of 24 km in the plan-view was sufficiently large to reduce any error due to model finite size to only a few percent. The model height averaged 7.5 km. The element size is variable. The largest zones were 400 m on edge horizontally by 200 m deep; the smallest, concentrated around the outcrop of the dike were 100 m horizontally by 50 m or more deep. The dike location, path and strike length are predetermined, not parts of the solution. The dike length in the plan-view was set at 4 km. Magma flow was confined to the single layer of zones of 50-m thickness (d). Magma was injected into the dike at the base at a rate of 0.45 m^2/s. The model was run until a steady state was reached with

magma exiting the top end of the crack. This was a purely mechanical calculation with no heat transfer.

The initial dike opening was 5 cm. The magma viscosity was 10 Pa·s, the density is 1141 kg/m^3. The vertical stress corresponded to an average rock-mass density of 2,400 kg/m^3. The far-field horizontal stresses were isotropic, equal to half the vertical stress. There was a "roller" boundary at the model bottom of the model, and the top was stress-free. A stress boundary condition in equilibrium with the overburden stress state was applied on the vertical model boundaries.

Results

Figure 2 shows the progress of magma at three successive times (later times are at the top). The model shows a negligible effect of topography when the magma front is about 2 km beneath the surface, the development of upward convexity of the magma front when the magma is less than 1 km beneath the surface at its centerline, and flow of magma out of the dike almost entirely to the right of the centerline when the magma reaches the surface. It is clearly seen that the main flow of magma is strongly diverted away from the topographic ridge.

The upper part of figure 3 depicts magma flow speeds in the upper 2 kilometers of the dike after eruption. The tendency for flow to concentrate toward the canyon end of the strike even at 4 km beneath the surface is clear. Any conduit forming on this dike will be located more than a kilometer from its centerline at depth and more than 2 kilometers from its edge under the ridge. The same concentration of flow toward the right-hand half of the dike is also seen in the dike aperture illustrated in the lower part of Figure 3.

One may question how much of this result is due to the increased overburden stress under the ridge and how much is simply due to the lower elevation of the canyon. Two associated calculations were done to address that issue. The upper plot in Figure 4 shows results with a flat upper surface but with an added surface load to reproduce the topographic overburden stresses (shown by the contours). This clearly shows a concentration of flow (indicated by arrows) to the right of the centerline. On the other hand, the lower part of Figure 4 shows the magma front and flow vectors that result if all of the rock in the upper four layers of fine zones is assigned a negligible density, removing any affect of topographic contribution to lateral confining stress on the dike. The results are very close to what is seen in the upper panel of Figure 2. Thus, it is concluded that both elevation and overburden stress variations contribute to diversion of the rising flow to the right, away from the ridge but that the larger contribution is the geometric one.

Discussion

The results above indicate that a dike rising from great depth near the transition from a lowland to a highland, and striking across that transition, will preferentially erupt toward the lowland and will avoid intrusion into the highland. The concentration of flow away from the ridge will result in concentration of advective heat flow in that region, maintaining low viscosities, which will in turn lead to a tendency for conduit localization in the lowland portion of the strike length of the dike, similarly to that described by Wylie et al. 1999.

The impetus for this calculation was to provide direction for the Probabilistic Volcanic Hazard Analysis of the proposed Yucca Mountain nuclear waste repository (CRWMS M&O, 1996). The repository is planned to be under Yucca Mountain, a fault block mountain in southern Nevada, USA. The mountain is the hanging wall on the east side of the north-south striking Solitario Canyon Fault, which underlies a canyon about 150 m lower than the crest of Yucca Mountain. The current state of stress is such that the maximum principal stress direction, which would be the expected strike of a future dike, is approximately N30W. Because all of the Pleistocene volcanic activity within 100 km of the mountain is found to the southwest in Crater Flat (Perry et al., 1998), it is of interest whether a dike centered under Solitario Canyon but extending to the northeast under Yucca Mountain would penetrate high enough into the mountain to threaten the repository, which would be located 200 to 300 m below the crest.

The topography used in our models represents a typical N30W transect of Yucca Mountain and Solitario Canyon. Figures 2 through 4 are views to the southeast, with Yucca Mountain on the left and Solitario Canyon on the right. Although the results show a clear tendency for flow to concentrate away from the ridge, the upper panel in Figure 2 clearly does show that magma still reaches elevations above the vent. However, the calculations indicate that magma will be moving very slowly (<0.2 m/s) and will be very thin (<20 cm) at its upper edge under the ridge. Such a slow moving, thin dike would likely solidify before penetrating far into this region (BSC, 2004).

There are many examples of basaltic eruptions localized on ridges rather than in adjacent lowlands; Sleeping Buttes is an example in the Yucca Mountain vicinity (Perry et al., 1998). These results do not preclude eruption out of a ridge. If the strike on the dike is

parallel to the length of a ridge, the effect described here will not operate. Another possibility is that the length of a dike may be so short that its strike does not extend far beyond the edge of the ridge.

Acknowledgements

This work was supported by the U.S. Dept. of Energy, Office of Civilian Radioactive Waste Management. Helpful suggestions were made by Greg Valentine. Any opinions are those of the authors.

References

BSC, 2004, "Dike/Drift Interactions" MDL-MGR-GS-000005 REV 01, Bechtel SAIC Company, Las Vegas, Nevada.

Brandsdottir, B. and Einarsson, P. 1979. Seismic activity associated with the September 1977 deflation of the Krafla central volcano in north-eastern Iceland. *J. Volcanol. Geotherm. Res.* ***6,*** 197-212.

CRWMS M&O 1996. *Probabilistic Volcanic Hazard Analysis for Yucca Mountain,Nevada.* BA0000000-01717-2200-00082 REV 0. Las Vegas, Nevada

Geertsma, J. and F. de Klerk, 1969. A rapid method of predicting width and extent of hydraulically induced fractures. *J. Petrol. Tech.* ***21***, 1571–1581.

Howard, G.C. and C.R. Fast, 1958, Optimum fluid characteristics for fracture extension. *Drilling and Production Practice.* Pages 261-270. Washington, D.C.: American Petroleum Institute.

Lister, J.R. 1990a. "Buoyancy-driven fluid fracture: Similarity solutions for the horizontal and vertical propagation of fluid-filled cracks." *Journal of Fluid Mechanics, 217,* 213-239.

Lister, J.R. 1990b. "Buoyancy-driven fluid fracture: The effects of material toughness and of low-viscosity precursors." *Journal of Fluid Mechanics, 210,* 263-280.

Lister, J.R. 1991, Steady solutions for feeder dykes in a density-stratified lithosphere. *Earth Planet. Sci. Lett.****107***, 233-242.

Lister, J.R. and R.C. Kerr, 1991. Fluid-mechanical models of crack propagation and their application to magma transport in dykes. *J. Geophys. Res.* ***96,*** 10,049-10,077.

Perkins, T.K. and L.R. Kern, 1961, Widths of hydraulic fractures. *Trans. Soc. Petrol. Eng. Amer. Inst. Min. Metall. Petrol. Eng.* ***222***, 937-949.

Perry, F.V., B.M. Crowe, G.A. Valentine and L.M. Bowker (eds.), 1998, *Volcanism Studies: Final Report for the Yucca Mountain Project*, Los Alamos National Laboratory report LA-13478, Los Alamos, NM, USA.

Pinel, V., and C. Jaupart, 2004, Magma storage and horizontal dyke injection beneath a volcanic edifice. *Earth Planet. Sci. Lett.****221***, 2245-262.

Pollard, D.D., P.T. Delaney, W.A. Duffield, E.T. Endo and A.T. Okamura, 1983, Surface deformation in volcanic rift zones. *Tectonophysics* ***94***, 541-584.

Pollard, D.D., and G. Holzhausen, 1979, On the mechanical interaction between a fluid-filled fracture and the earth's surface. *Tectonophysics* ***53***, 27-57.

Pollard, D.D., and O.H. Muller, 1976, The effects of gradients in regional stress and magma pressure on the form of sheet intrusions in cross section. *J. Geophys. Res.* ***81***, 975-984.

Rubin, A.M., and D.D. Pollard, 1988, Dike-induced faulting in rift zones of Iceland and Afar. *Geology* ***16***, 413-417.

Rubin, A.M., 1990, A comparison of rift-zone tectonics in Iceland and Hawaii. *Bull. Volcanol.* ***52***, 302-319.

Rubin, A.M., 1992, Dike-induced faulting and graben-subsidence in volcanic rift zones. *J. Geophys. Res.* ***97***, 1839-1858.

Spence, D.A., and D.L. Turcotte, 1985, Magma-driven propagation of cracks. *J. Geophys. Res.* **90,** 575-580.

Spence, D.A., and D.L. Turcotte, 1990, Bouyancy-driven magma fracture: A mechanism for ascent through the lithosphere and emplacement of diamonds. *J. Geophys. Res.* ***95,*** 5133-5139.

Wylie, J.J., K.R. Helfrich, B. Dade, J.R. Lister, and J.F. Salzig, 1999, Flow localization in fissure eruptions. *Bulletin of Volcanology, 60,* (8), 432–440.

Zhang, X., R. Jeffrey, and E. Detournay (2002). NPHF2D, Non-Planar Hydraulic Fracture 2D User's Manual. Melbourne, Australia: CSIRO Petroleum.

Figure Captions

Figure 1. Schematic of the hypothesis that magma in a dike rising under a canyon adjacent to a mountain will not reach a position under the mountain even if that level is at a lower elevation than the bottom of the canyon. Shaded region below solid arc represents magma.

Figure 2. Perspective views of plane containing dike and topography behind showing magma rising in dike. Dike is restricted laterally to the 4-km wide region in color. Colors indicate the volume percentage of magma in the zone; orange >90%, blue < 10%, so green is approximate location of magma front. Arrows indicate magma discharge (velocity integrated over thickness) vectors; maximum discharge is 1.25 m^2/s (that is 1.25 m^3/s per meter of strike length). From bottom to top: magma is ~2,000 meters below surface; magma is less than 1 km beneath surface; magma has reached the surface ~1½ km farther SW than its midpoint along strike.

Figure 3. Top: Plot showing contours of magma velocity magnitudes (max = 3.1 m/s; colors: red > 3.0 m/s, in 0.25-m/s steps, dark blue < 0.5 m/s) and discharge vectors (as in Figure 2, but reduced in scale) as magma reaches the surface. The effect of the surface can be seen even at the bottom edge of the plot (about 2 km beneath the surface). Bottom: Contour plot of dike aperture at end of simulation showing greatest dike apertures (max = 0.72 m; colors: red >0.7 m, in 0.05-m steps, dark blue < 0.15 m) are deflected toward the lower topography.

Figure 4. Top: Results for a flat surface with topographic stresses from earlier model imposed. Contour plot shows imposed vertical stresses (greyscale outside of dike, colors in dike; red < 10 MPa, in 10 MPa steps, darker greeen >50 MPa). Arrows show magma discharge vectors (max = 0.9 m^2/s) which are deflected to the right by only ~ 0.8 km in the absence of surface roughness or tilt. Bottom: Compare with the top portion of Figure 2. Results for a model with surface topography but without topographic stresses above lowest surface point along dike. Contour colors indicate volume percentage of magma in zone as in Figure 2.

Figure 1.

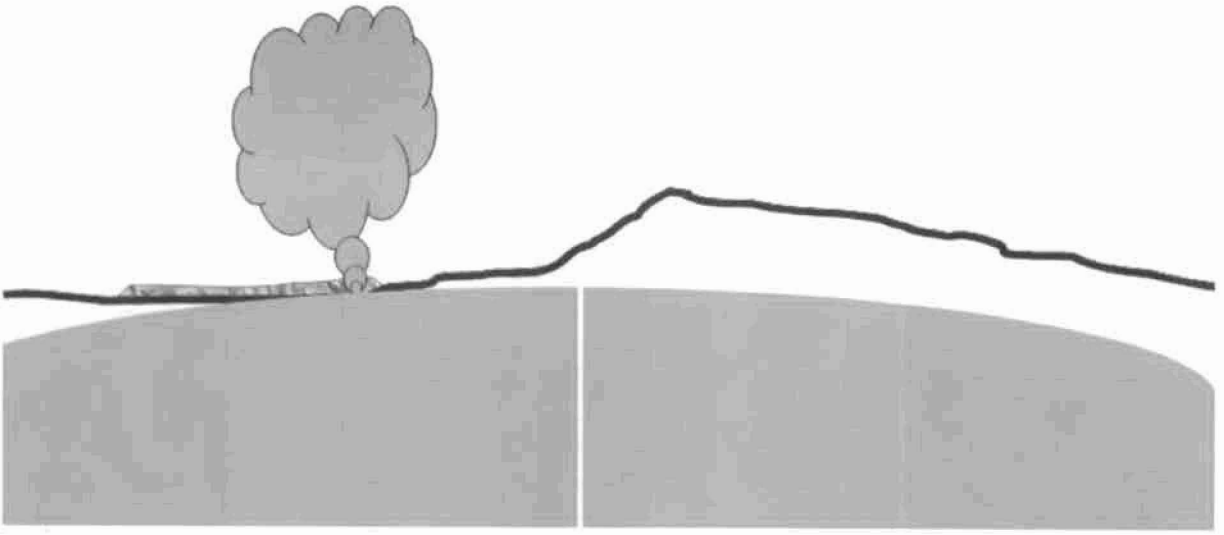

Figure 2.

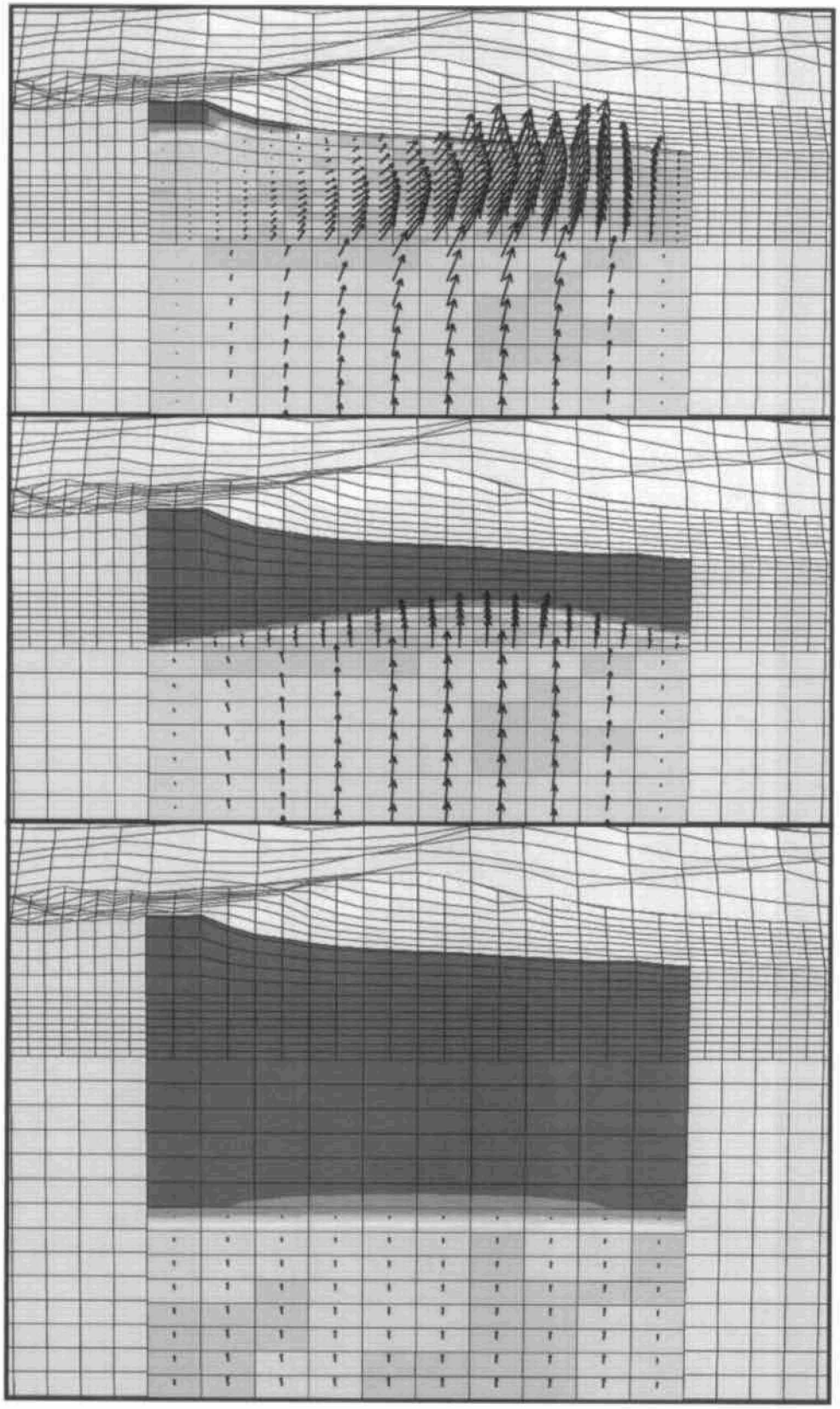

Figure 3.

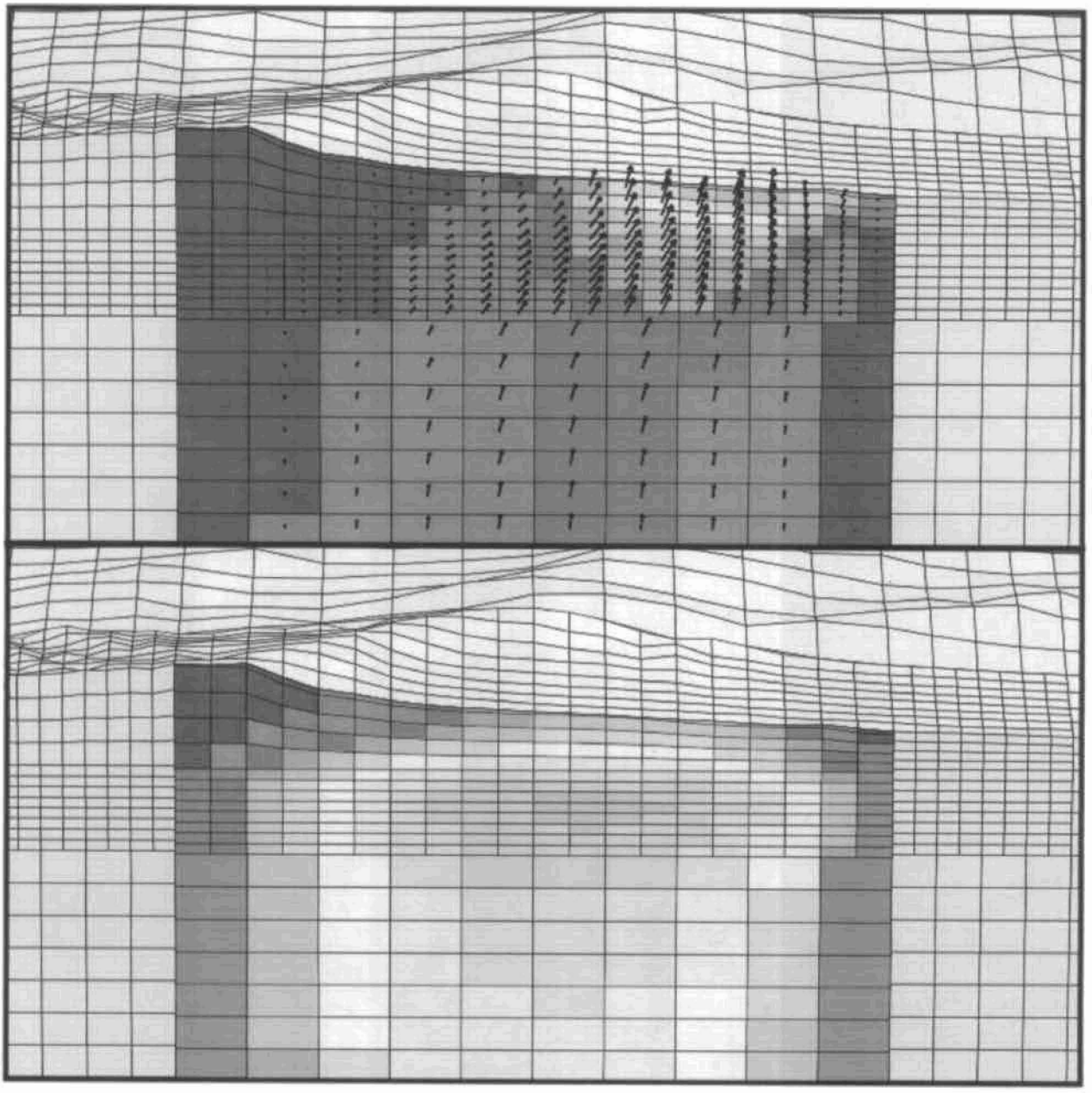

Figure 4